2024

CHARACTERIZING SEX DIFFERENCES IN HPV NEGATIVE HEAD AND NECK SQUAMOUS CELL CARCINOMA

Sarah Barclay

CHARACTERIZING SEX DIFFERENCES IN HPV NEGATIVE HEAD AND NECK SQUAMOUS CELL CARCINOMA

By

Sarah Barclay

B.A., Concordia College, 2019

A Thesis Submitted in Partial Fulfillment of
the Requirements for the Degree of Master of Science

Division of Basic Biomedical Sciences

Basic Biomedical Sciences Program
In the Graduate School
The University of South Dakota
May 2024

The members of the Committee appointed to examine
the Thesis of Sarah Barclay
find it satisfactory and recommend that it be accepted.

DocuSigned by:
Kurt Warnhoff
5567A6EF70D749D...
Chairperson

DocuSigned by:
Paola Vermeer
C38D8628E3784AD...

DocuSigned by:
Robert Morecraft
D3B90C4695EF499...

ABSTRACT

It is now widely accepted that peripheral solid tumors are infiltrated by nerves. This infiltration of malignancies by nerves is referred to as tumor innervation. The Vermeer laboratory studies tumor innervation primarily in head and neck squamous cell carcinoma using a syngeneic cell line representing a mutationally-induced form of the disease; these cells are called MOC2-7 cells. In addition to defining the molecular consequences of tumor-infiltrating nerves on disease, the lab also focuses on their influence on behavior. This is important as cancer patients have a significantly higher incidence of depression and anxiety as compared to the population at large. In humans, males are more susceptible to head and neck cancers than females, thus few studies have analyzed this disease using female animals. To assess the impact of tumor-infiltrating nerves on disease, MOC2-7 cells were orthotopically implanted into the mouse oral cavity and tumor growth, innervation, and cancer-associated behavioral changes in female mice were characterized and compared to their male counterparts. We found that MOC2-7 tumors grow significantly slower in females. Surprisingly, tumors were also significantly more innervated in females. However, there were no differences in behavioral decline between tumor-bearing males and females. These findings suggest that nerve recruitment may differ between males and females. Treatment of tumors with cisplatin and radiation, standard-of-care treatment for HNSCC patients, slowed tumor growth for both male and female mice. Interestingly, tumors from treated mice were also significantly more innervated compared to untreated mice, with females having a greater increase in nerve density. Moreover, treatment did not appear to improve tumor-associated behavior changes. The tumor-brain circuit did not differ between males and females, regardless of treatment, indicating that the observed changes of increased innervation only had a local impact on the tumor. Head and neck cancer patients often receive the same treatment regardless of sex. From our studies, it is clear that sex has an influence on tumor growth and innervation, and that treatment may exacerbate tumor innervation. Thus, it is important that we, as a field, continue to study this disease in the female population.

Thesis Advisor Dr. Paola Vermeer 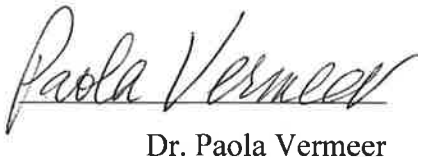

Dr. Paola Vermeer

ACKNOWLEDGEMENTS

I am forever grateful to my wonderful, kind, and supportive mentor, advisor, and friend, Dr. Paola Vermeer. From assisting me in designing experiments, to helping me decide my academic career path, to attending my wedding, she has been there with caring support every step of the way. Regardless of where my future stands and career take me, I am certain that as I reflect back on my academic development, Dr. Vermeer will have been one of the most important influences along my journey.

Many thanks to my colleagues in the Vermeer lab, Austin Walz, Jeffery Barr, and Tony Restaino, for teaching me all I have learned, to the members of the Spanos lab, Dr. Chad Spanos, Craig Welbon, and Payal Ghosh, and to Caitlin Williamson, for helping with anything I may have needed. I truly appreciate all the great times we had and memories we have made.

A huge thank you to all of my fellow graduate students. I could not have made it through without your undeniable friendship, love, and encouragement.

Finally, I would like to thank my family. To my parents, thank you for all of your love and support through every step of this journey. Mom, thank you for always being willing to dog-sit and supply dinner. Planning a wedding is difficult enough, let alone during graduate school, and I couldn't have done it without you. Dad, thank you for all the advice you have given me throughout the years. From writing, to career choices, to interviewing, you've never steered me wrong. A very special thank you to my husband, Andrew. Thank you for undying love and support throughout my time as a graduate student. I know the road was long with its many ups and downs. With every rant, every tear, every time I felt like quitting, you were there for me. And a thank you to my dog Willow, the best distraction from the stress and pressure of graduate school.

TABLE OF CONTENTS

LIST OF FIGURES

INTRODUCTION

The influence of nerves within malignancies has been specifically studied for only the past decade, though their association with cancer has been appreciated since the 1890s [1]. Electrophysiologic studies show that tumor-infiltrating nerves remain functional at the tumor bed while molecular studies indicate the nerve released factors (e.g., neurotransmitters, neuropeptides) impact disease progression via direct and indirect mechanisms [2-4]. Published studies evaluating gender in the context of cancer indicate the presence of sex differences. For example, males with gastric cancer suffer a worse prognosis than females; moreover, being male was an independent poor prognostic risk factor [5]. On the other hand, women with bladder cancer suffer a worse prognosis and survival as compared to their male counterparts [6]. Thus, different patient outcomes correlate with gender in different cancers. Analysis of cancer incidence using the Surveillance, Epidemiology, and End Results (SEER) database, demonstrated significantly different incidences of the many cancers in males and females [7]. Despite these findings, the majority of studies in the emerging field of cancer neuroscience have utilized only male mouse cancer models or combine data from males and females [8]. Thus, the current literature limits the understanding of sex as a biological factor in tumor innervation and/or its influence on disease.

Head and neck squamous cell carcinoma (HNSCC) are cancers that arise in the oral cavity, the oropharynx and the larynx. While predominantly a male cancer [9], the incidence of HNSCC in females cannot be ignored. Interestingly, females with HNSCC have a better prognosis [10] than males. Whether cancer-associated nerves contribute to this better outcome is not known. Importantly, using a syngeneic model of HNSCC, we have mapped tumor-infiltrating nerves and found they associate with a pre-existing circuit that connects to specific regions in the brain [11]. Neurons within this circuit are transcriptionally and functionally altered resulting in behavioral

changes. Importantly, HNSCC patients suffer with a higher incidence of mental health decline as compared to the non-cancer population at large [12, 13]. This decline is maintained even after standard-of-care therapy [14]. Whether tumor-infiltrating nerves via their connection to the brain contribute to the mental health decline in cancer patients is not known. Moreover, the process of tumor innervation likely has already occurred by the time patients experience symptoms, receive a cancer diagnosis and commence treatment. Thus, it also becomes important to define the influence of standard-of-care treatments on tumor-infiltrating nerves and the impact on behavior. Currently, no studies have addressed these key issues.

Tumor innervation

The presence of nerves in various peripheral tumors, including those from breast, uterus, bone, and neck tissues, was first discovered in 1897 with methylene blue staining [1]. However, since then the impact of tumor-infiltrating nerves on cancer has been greatly understudied. A few studies emerged in the early 1900s with evidence supporting the idea that nerves could infiltrate tumors [15]. Only over the past decade have we come to appreciate the influences of tumor innervation on cancer initiation and progression. Convincing data implicating tumor-infiltrating nerves in cancer emerged in the early 2000s and included esophageal cancer, fibrosarcoma, and pancreatic cancer [16-18]. Immunohistochemical (IHC) staining of breast, prostate, pancreatic, lung, liver, ovarian, colon, head and neck, and melanoma patient tumors for the neuronal marker, β-III-tubulin, revealed the presence of nerve twigs and nerve bundles [19]. This suggests that most, if not all, peripheral malignancies are innervated.

Head and neck squamous cell carcinoma

Head and neck squamous cell carcinomas account for 4.5% of cancers worldwide [20]. These cancers can be are broadly divided into two categories. The smaller group of cases are associated with infection with high-risk human papillomavirus (HPV+) while the larger cohort (approximately 80%) are instead associated with the risk factors of smoking cigarettes and drinking alcohol (HPV-) [21]. While the rates of cigarette smoking continue to decline (predominantly due to public awareness of the hazards of smoking), the incidence of HPV infection is at epidemic proportions. Thus, the incidence of HNSCC is on the rise [22] [23-25]; in fact, it is predicted that the incidence of HNSCC will increase by 30% in 2030 making this cancer a public health concern. HNSCCs are cancers that arise in the oral cavity, oropharynx and larynx. HNSCC patients suffer one of the highest mortality rates [20, 26] for all cancers. Moreover, while cure rates for HPV+ HNSCC are generally high, the majority of all (HPV+ and HPV-) patients experience metastasis which is rarely cured.

Cancer and mental health decline

A cancer diagnosis often entails significant mental health changes. Major depression, for instance, affects 20-50% of cancer patients, varying by study and cancer type [27-31]. Cancer patients with depression have a higher mortality rate compared to non-depressed patients [32-34]. Even long-term survivors (over 10 years) experience a higher rate of depression (12%) compared to the population at large [14, 35]. The connection between cancer and depression, whether due to the disease itself or its treatment, remains unclear. However, it suggests that cancer may alter brain functions. These changes might be driven by substances released by cancer cells or damaged cells from therapy, or through neural mechanisms of communication between the tumor and the brain.

Female patients with HNSCC have improved outcomes compared to males [36]. While this correlation is complex as race also contributes to outcomes, this difference indicates that studies assessing the influence of gender in HNSCC will provide critical information that may influence disease treatment. It remains unknown whether the number and/or type of tumor-infiltrating nerves or the impact of treatment on them contributes to the influence of gender in patient outcomes. This project aims to fill this critical gap in knowledge.

MATERIALS AND METHODS

Cell lines

The mouse oral carcinoma (MOC) 2-7 cell line has been previously described [37]. Cells were maintained in Dulbecco's Modified Eagle Medium (DMEM) with 10% fetal bovine serum (FBS) at 37°C with 5% CO2.

Animal studies

Male and female 8-9 week old C57Bl/6 mice were purchased from The Jackson Laboratory. Mice were acclimated to the facility for 2 weeks prior to the start of any study. Mice were ear-notched for identification.

Study approval

All animal studies were performed in the Sanford Research Animal Resource Center (ARC) with approval from the Institutional Care and Use Committee at Sanford Research; all studies complied with all relevant ethical regulations and were within institutional guidelines. The Animal Welfare Assurance number on file for Sanford Research is A-4568-01 and it is AAALAC, Intl accredited.

In addition, Sanford Health is licensed with the United States Department of Agriculture (USDA) as a research facility with USDA certificate number 46-R-011. The ARC is a pathogen-free facility and mice are maintained in IVC Tecniplast Green line Seal Safe Plus cages; cages are opened under aseptic conditions within an animal transfer station. Cage changes occur every other week and are performed using aseptic technique. All cages receive HEPA-filtered air and animal rooms are maintained at 75°F with 30-70% humidity. Cages receive a minimum of 15 air changes/hour and are maintained under a 14:10 light:dark cycle. Nesting materials and corncob bedding are provided and autoclaved prior to use. Food consists of irradiated sterile Envigo pellets while water is acidified (pH 2.8-3.0); both provided ad libitum. There is a maximum of 5 mice/cage and they are observed on a daily basis by ARC technicians as well as laboratory staff for signs of distress or illness. Mice undergoing behavioral analysis were individually housed.

Tumor cell implantation

MOC2-7 cells were grown and passaged at least twice in antibiotic-free media prior to implantation. Cells were washed twice with 1x phosphate buffered saline (PBS) then trypsinized with 0.05% trypsin for 5 minutes. Trypsin was inactivated with PBS containing 2% FBS. Cells were centrifuged at 300x g for 5 minutes. Cells were diluted in pure DMEM to the appropriate cell concentration/volume for injection. For all tumor injections, a cell concentration of 50,000 cells per 50µl was used. Cells were kept on ice until injections.

Mice were fully anesthetized with an 87.5mg/kg Ketamine and 10mg/kg Xylazine cocktail using a 27-gauge insulin needle via intraperitoneal injection. Mice were kept in empty recovery cages on heating pads and eye ointment applied to keep their eyes from drying out. The cell solution was manually inverted to ensure an even distribution of cells and drawn up into a 1ml syringe. Once fully anesthetized, mice were injected one at a time. Forceps were used to pull the lip away from

the injection site and a 25-gauge needle was inserted bevel-side up and perpendicular into the back corner of the mouth into the cheek pouch, behind the whisker pad. The needle was inserted deep enough so that only the bevel was inside the tissue, then 50µl of the cell solution was slowly infused. Mice were returned to their home cages once fully awake.

Tumor growth

To measure tumors, mice were briefly anesthetized with isoflurane. Tumors were measured with digital calipers for length and width (mm). Tumor volume was calculated with the formula: Volume = ½ (length*width2). Tumor growth was limited to 1000mm3. Weight loss began after tumors surpassed 500mm3, during which soft food was introduced on the cage floor to encourage eating.

Behavior assays

Mice were acclimated to being individually housed for two week prior to the start of behavior testing. During this time, mice were handled on at least three separate occasions by scruffing for 30 seconds then held in an open palm for 30 seconds. This acclimated the mice to handling.

Nest building and burrowing: Nest building and burrowing are innate rodent behaviors of both sexes and are general indications of well-being. To assess nesting behavior, mice were individually housed and provided with a square nestlet overnight, from which they would shred and build a nest. The following morning the nests were scored on a scale of 0 to 4 by two independent scorers blinded to the conditions. Scoring of nests is standardized; a score of 0 indicates the mouse did not touch the nestlet at all, 1 indicates the mouse shredded less than 50% of the nestlet, 2 indicates the mouse shredded greater than 50% of the nestlet but the nest is less and half the body height of the mouse, 4 indicates the mouse shredded over 50% of the nestlet and the nest is greater than half its body height [38]. Mice were exposed to the cotton nestlet twice during their two-week acclimation

period to being individually housed to ensure they were able to shred the nestlets. Three baseline tests were given before tumor implantation. The average of the three baseline tests were taken, and any mouse that did not average above a score of "3" was excluded from the data set.

To assess burrowing behavior, mice were tasked with removing corncob bedding from a slightly elevated tube within 30 minutes. Mice acclimated to the room prior to the start of the test. The weight of the bedding in the tube was recorded before and after the test [39]. Three baseline tests were given prior to tumor implantation, and the average of those three tests was taken. Both sexes were able to successfully remove the corncob bedding, though it appeared the females preferred to leave a bit more behind in the tube.

Open field test: The open field test is designed to measure locomotor activity [40]. This assay was performed in a dimly lit room to reduce stress induced from a bright light. Mice acclimated to the room for 20 minutes prior to testing. Mice were placed in a box (16"x16"x13.5) with enclosed walls with a camera is set up above the box to record the mouse's movements using the AnyMaze software. Boxes were cleaned after each use.

Voluntary wheel running activity: Voluntary wheel running measures physical performance and endurance. Fatigue-like behavior emerges as decreased wheel running [41]. Mice were individually housed in cages with free access to running wheels that wirelessly transmitted data to a hub to continuously monitor time spent running and the distance run each day (Low-Profile Wireless Running Wheel, MedAssociates Inc.). Wheels were removed on nights of the nesting test, and returned the next morning after being cleaned with warm soapy water and sanitized with 70% ethanol.

Chemotherapy & Radiation of oral tumors

Chemoradiotherapy was performed simultaneously, once per week for two weeks (on days 14 and 21 post-tumor implantation). Mice were first anesthetized with an 87.5mg/kg Ketamine and 10mg/kg Xylazine cocktail. Once anesthetized, mice were given an intraperitoneal cisplatin injection (5.28 mg/kg). Cisplatin was mixed with PBS and kept in the dark until injections.

Radiotherapy treatment consisted of 8 Gy of radiation. Anesthetized mice were placed in individual lead-lined shielding devices with only the tumor facing up and exposed. Mice were held in place gently with medical tape. Lead tape was used to adjust the size of the hole depending on the size of the tumor to ensure that only tumor was exposed to radiation. Anesthetized mice within their shielding devices were then carefully placed inside the irradiator (RS-2000, RadSource) and exposed to 8Gy X-ray radiation. After irradiation, mice were injected subcutaneously with 100µl saline to prevent dehydration. Untreated mice were given the same anesthesia required for radiation treatment, and 100µl saline. Mice we kept in recovery cages on heating pads until fully awake, after which they were returned to their home cages.

Nerve Tracing

Mice were briefly anesthetized with Isoflurane. Wheat Germ Agglutinin (WGA) linked to A568 was injected intra-tumorally (2µl) using a Hamilton syringe. Mice were left in their cages for 5-7 days to allow retrograde transport of the tracer before euthanasia.

Tissue collection & fixation

When euthanasia criteria were reached (as indicated in the approved IACUC protocol), animals were euthanized with CO2 followed by cardiac perfusion with PBS followed by 10% formalin. The tumor, lungs, lymph nodes, brain, and trigeminal ganglia were collected and fixed in 10%

formalin for at least 24 hours. Tissues were then transferred to PBS; brains were transferred to 30% sucrose.

IF staining

Tumors were embedded in paraffin, sliced (4 μm), and mounted onto glass slides. To dewax, slides were soaked in Xylene for 5 minutes with agitation every 30 seconds, followed by a series of 1-minuted washes of 100%, 90%, and 70% EtOH. Slides were briefly washed in H2O for 1 minute before being transferred to pre-warmed antigen retrieval buffer (10mM sodium citrate, 0.05% Tween 20, pH 6.0) for 30 minutes covered in a 95°C water bath and 20 minutes uncovered at room temperature, after which they were washed in running water for 5 minutes. Slides were dried and a ring was drawn around tissue with an Immedge pen. PBS was used to keep the tissue from drying out. Slides were blocked with blocking buffer (3% goat serum, 1% BSA, in PBS) with 0.01% TX-100 for 30 minutes at room temperature. Slides were washed 3x for 5 minutes with PBS. Sudan B (diluted 1:20 in 70% EtOH) was applied for 30 seconds to 1 minute, followed by PBS washes (3x 5 min). Slides were incubated in primary antibody diluted in blocking buffer (1:500) in a humidified chamber overnight at 4°C. Slides were washed 3x for 5 min with PBS and incubated in secondary antibody, diluted in blocking buffer (1:500) in a humidified chamber in the dark for 1 hour at room temperature. Slides were washed 3x 5 min with PBS. For single antibody staining, slides were then incubated in Hoechst (1:10,000 in PBS) and washed 2x 5 min in PBS. For dual staining with antibodies of the same host species, conjugated antibody diluted in blocking buffer (1:500) was applied, and slides incubated in a humidified chamber overnight in the dark at 4°C, followed by Hoechst incubation and washes. Glass coverslips were mounted with Fluoromount-G Mounting Medium. Staining was analyzed using a confocal microscope (Nikon A1 TIRF). For

each tumor, three to four images were taken on the confocal microscope at 20x for representative areas nerve twigs and nerve bundles.

ImageJ Analysis

Z-stacks collected on the confocal were opened as a hyperstack. The target channel was isolated and the z-stack was compressed to a maximum intensity image. The lowest threshold was set and used for all images. The total area of the positive staining (nerves) was measured. If nerve bundles were present, they were traced and an ROI was created. The area of the nerve bundle was measured and subtracted from the total area.

Statistics

Statistical analysis for tumor growth included non-linear exponential growth curve and repeated measures ANOVA. Analysis for tumor innervation and nerve density included student's T-test with Welch's correction when comparing two groups of different sample sizes. For nesting, burrowing, and open field analysis, sexes were compared using student's T-test with Welch's correction for each time point. Student's T-test was also used to compare each time point to baseline for each sex. For running wheel behavior analysis, repeated measures ANOVAs were used to compare differences between sexes over time.

RESULTS

MOC2-7 tumors grow slower in female mice

To determine whether sex influences tumor growth, MOC2-7 cells were implanted in 8-9 week old male and female C57BL/6 mice (n=10 per group). Tumor growth was measured weekly with digital calipers. Interestingly, MOC2-7 tumors grew significantly slower in female mice (Figure 1A). To determine if the smaller tumor sizes is due to the smaller body size of female mice, tumor volume was normalized to body weight at each time point and the tumor growth curves re-plotted (Figure 1B). When body weight was taken into account, tumors remained significantly smaller in female mice.

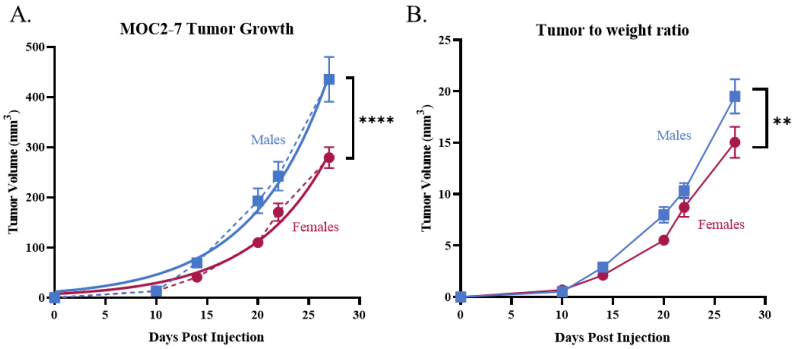

Figure 1. Tumor growth curves. A) Growth of MOC2-7 tumors in male (blue) and female (red) mice (n=10 per group) Tumor growth plotted (dotted lines) with non-linear exponential growth curve (solid lines). Statistical analysis by repeated measures ANOVA, $p<0.0001$ B) Tumor volume normalized to body weight, plotted as a ratio. Statistical analysis by repeated measures ANOVA, $p=0.0051$.

Tumors in female mice are more densely innervated

We have previously demonstrated that densely innervated tumors grow faster than those that are sparsely innervated [4]. However, this study was performed using only male mice. Thus, to compare the innervation density between male and female tumors, MOC2-7 oral tumors were implanted in male and female mice, harvested and immunofluorescently stained for β-III tubulin (a pan neuronal marker). Given that MOC2-7 tumors grow slower in females, we were surprised to find that these tumors were significantly more innervated as compared to their male counterparts (Figure 2A). When innervation density was normalized to tumor volume, female tumors remained significantly more innervated than male tumors (Figure 2B). Taken together, these data indicate that female mice have smaller, yet more densely innervated tumors as compared to males.

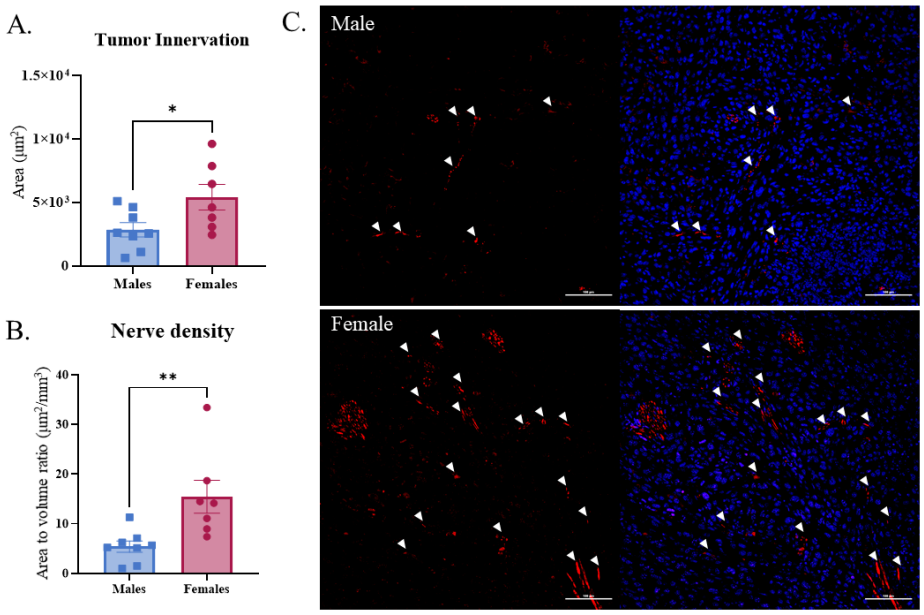

Figure 2. Tumor innervation of MOC2-7 tumors in male and female mice. A). Images were quantified using ImageJ software for the total area (mm^3) of positive β-III tubulin staining. Average area was calculated from 3-4 images per tumor (n=7-8 per group). Students T-test, p=0.0282. B) Average nerve area (mm^2) divided by tumor volume (mm^3). Student's T-test, p=0.0097. C) Representative pictomicrographs of β-III tubulin-stained nerve twigs (red, arrows), Hoechst (blue). Scale = 100µm.

We have previously determined that MOC2-7 tumors in male mice are innervated with TRPV1 expressing sensory nerves [11]. To determine the type of nerves infiltrating MOC2-7 tumors in

females, tumors were immunofluorescently stained for β-III tubulin as well as TRPV1 (sensory marker), tyrosine hydroxylase (TH, sympathetic marker) and vasoactive intestinal polypeptide (VIP, parasympathetic marker). Quantification of fluorescence intensity for each of the neuronal markers shows that, similar to their male counterparts, female MOC2-7 tumors are innervated by TRPV1 expressing sensory nerves (Figure 3).

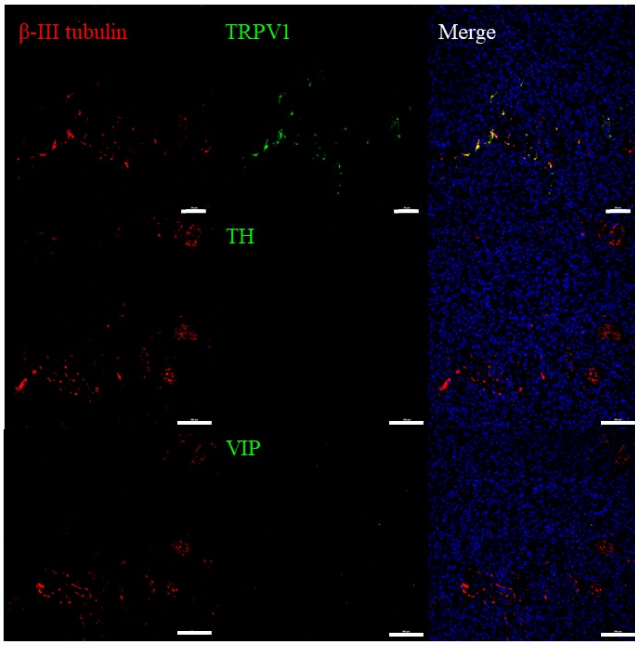

Figure 3. Nerve subtypes in female tumors. Tumors (n=3) were immunofluorescently co-stained for β-III tubulin (red) and TRPV1, TH, or VIP (green), Hoechst (blue). Three to four images were taken on the confocal microscope at 20x magnification for representative areas of nerve twigs and nerve bundles. Scale = 100μm.

The presence of nerves within cancers has also been documented in other peripheral malignancies [19, 42-45]. Moreover, direct and indirect neural effects on disease progression have been described. For example, release of Calcitonin Gene Related Peptide (CGRP), a neuropeptide by sensory neurons, binds the RAMP1 receptor which is expressed by cytotoxic CD8+ T cells. This interaction results in the inactivation of CD8+ T cells [2], a critical population of anti-tumor immune cells, and indirectly promotes tumor growth. Sensory neurons also release Substance P. This neuropeptide binds its receptor, NK1R, which is expressed on tumor cells and directly promotes tumor cell proliferation as well as migration [4]. In this way, tumor-infiltrating nerves promote tumor growth and disease progression.

A recent study shows that the neural influence on cancer extends beyond the tumor bed. Specifically, in mice bearing oral HPV negative malignancies, tumor-infiltrating nerves connect to a pre-existing circuit that projects from the tumor bed, to the ipsilateral trigeminal ganglion and

into specific regions in the brain. Importantly, microarray analysis shows that tumor-infiltrating neurons undergo transcriptional alterations and that these changes are reflected in significantly heightened calcium activity. The culmination of these cancer-induced neuronal changes is reflected in altered behavior [11].

The tumor-brain circuit does not differ between males and females

Neural tracers are molecules (typically fluorescently labeled) that are taken up by nerve terminals and transported (retrogradely or anterogradely, depending on the tracer). Previous published studies have demonstrated that neuronal tracers can be utilized to identify circuits connected to tumor-infiltrating nerves. Interestingly, intra-tumoral injections not only identify neuronal circuits associated with tumors but found that these circuits include regions in the brain [11, 46]. The Vermeer lab has shown that oral MOC2-7 tumors in male mice are innervated by nerves that connect to the V3 branch of the ipsilateral trigeminal (TGM) ganglion and connect further with the spinal nucleus of the trigeminal (SpVc), the parabrachial nucleus (PBN) and the central amygdala (CeA) [11].

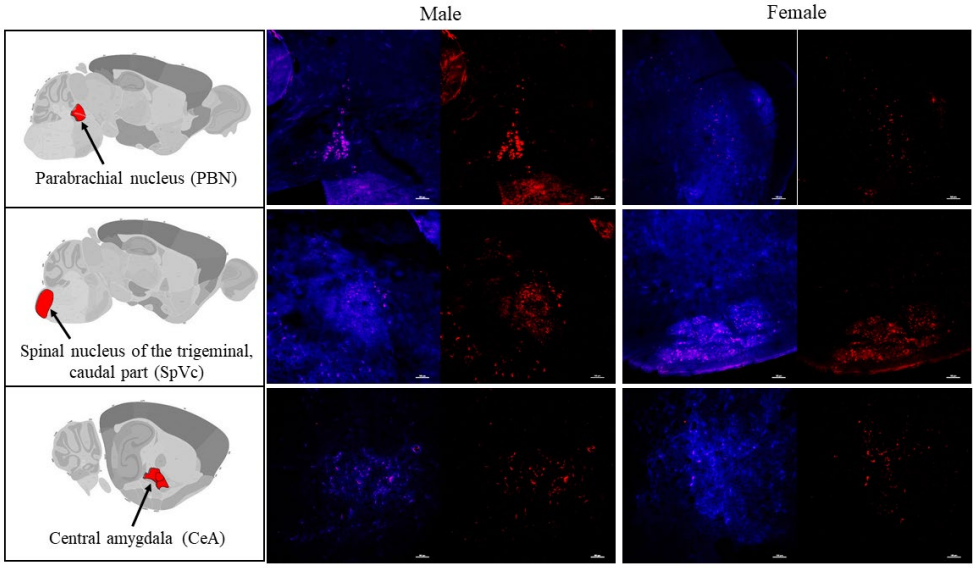

Figure 4. Neural tracer positive brain regions. Positive WGA neural tracer found in the PBN, SpVc, and CeA in both male and female tumor-bearing animals (n=4). 10x magnification, scale = 100μm. Diagrams from Allen Reference Atlas – Mouse Brain, atlas.brain-map.org.

To determine if this tumor-brain connection differs between sexes, MOC2-7 oral tumor-bearing mice (n=4 per group) were intra-tumorally injected with tracer and euthanized 5-7 days later (ensuring ample time for the tracer to reach the brain). Brains were harvested and sections analyzed by confocal microscopy for the presence of tracer. As mentioned, tumor-infiltrating nerves connect MOC2-7 tumors to the TGM, SpVc, PBN and CeA. Importantly, these same regions were tracer positive in females bearing MOC2-7 oral tumors, indicating that the tumor-brain connection does not differ between sexes (Figure 4).

Tumor-associated changes in behavior do not differ between sexes

Given these findings, we next asked whether cancer-associated behavioral changes differ between the sexes since tumor-bearing females harbor densely innervated disease. To address this question, three behaviors were assessed in tumor-bearing male and female mice: nesting, burrowing, and open field. Nesting is a measure of wellbeing in mice and is an innate behavior of males and females [38]. Similarly, burrowing, another innate rodent behavior, is also used to assess wellbeing [39]. Finally, open field test was used as a general measure of exploration activity [40]. Prior to tumor implantation, mice underwent behavioral testing and baseline behaviors were recorded. Following tumor implantation, behavioral assessments were completed weekly.

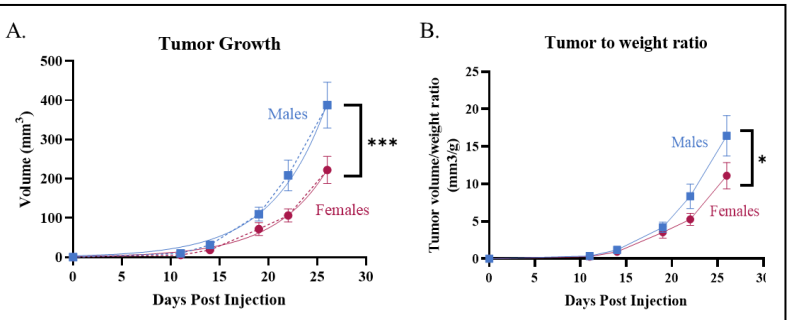

Figure 5. Tumor growth curves. A) Growth of MOC2-7 tumors in male (blue) and female (red) mice (n=11-12 per group) Tumor growth plotted (dotted lines) with non-linear exponential growth curve (solid lines). Statistical analysis by repeated measures ANOVA, p=0.0002. B) Tumor volume normalized to body weight, plotted as a ratio. Statistical analysis by repeated measures ANOVA, p=0.0235

Interestingly though females have slower growing and, therefore, smaller tumors (Figure 5 A, B), there were no statistically significant differences in behavioral changes between the sexes. Some mice of both sexes had abnormally slow growing tumors not appearing until day 18 post-implantation. Though we are unsure as to why these tumors grew slower, it is possible that this was due to poor cell injections. These mice with slow growing tumors were excluded from analyses.

Nesting behavior in male mice started to decline after post-tumor implantation day 12. Compared to baseline, statistically significant differences were seen at day 25, indicating a decline in nesting behavior over the course of the disease. Nesting behavior in females similarly declined and were not significantly different from their male counterparts (Figure 6A, B).

Likewise, the decline in burrowing behavior was similar for males and females, and did not commence to decrease until day 26 post-tumor implantation. For both sexes, compared to baseline, significant differences were not present until day 34, indicating there was only a slight decline in burrowing behavior over the course of the disease. When comparing individual time points between males and females, it appeared that there were significant differences in baseline behavior and early time points, however this difference disappeared as time went on. We suspect this is due to the females needing more time to acclimate to the burrowing assay task (Figure 6C, DB).

In the open field test, females demonstrated a higher total distance traveled, however, it was not significantly different from males. As the disease progressed, the rate of decline in total distance traveled was the same for both sexes (Figure 6E, F). It is important to note that the decline in total distance travelled may reflect mice acclimating to the box and thus, less willing to explore at each successive time point tested. The time spent in various zones, termed wall, middle, and center, was

also measured. While female mice gradually spend more time along the wall compared to males, this was not statistically significant (Figure 6G).

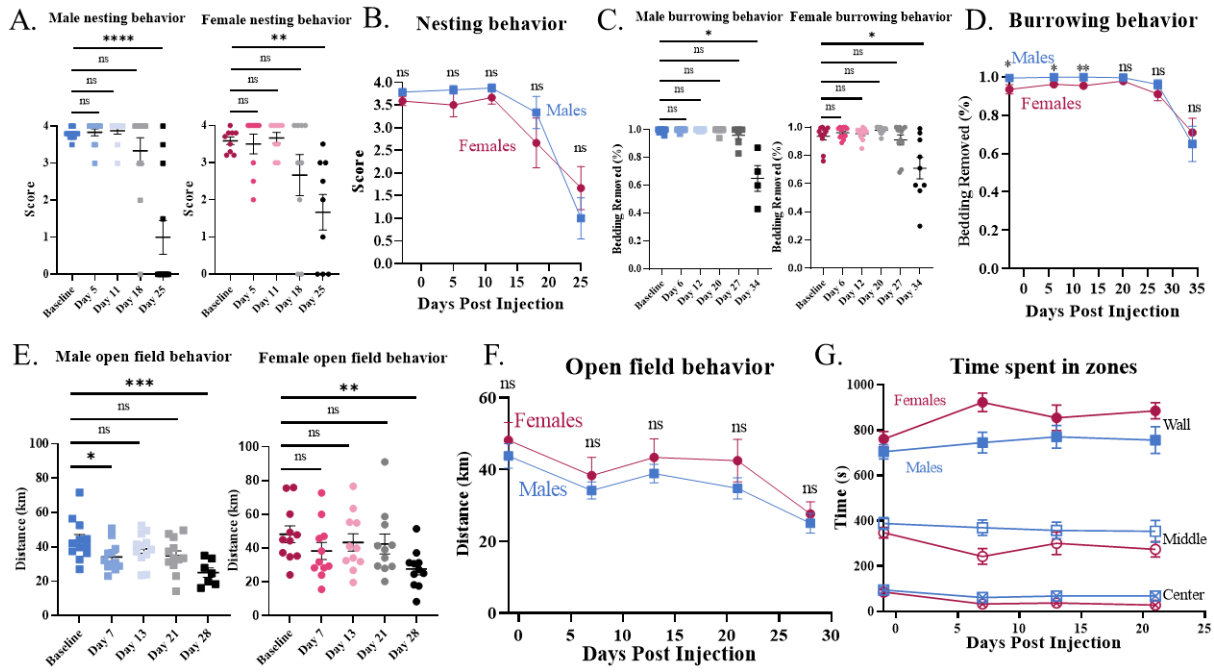

Figure 6. Behavioral assays for male and female tumor-bearing mice. A) Male and female nesting behavior scores. Student's T-test, statistically significant at day 25, males p <0.0001, females p= 0.0012. B) Nesting behavior of both sexes over time. Student's T-test with Welch's correction at each time point. C) Male and female burrowing behavior. Student's T-test, statistically significant at day 34, males p=0.0335, females p= 0.0182. D) Burrowing behavior for both sexes over time. Student's T-test with Welch's correction at each time point, statistically significant at baseline, day 6, and day 12, p= 0.0398, 0.0131, 0.0062, respectively. E) Male and female open field behavior. Student's T-test, statistically significant for males at baseline and day 28, p= 0.0317, 0.0005, respectively; and for females at day 28 p= 0.0031. F) Open field behavior for both sexes over time. Student's T-test with Welch's correction at each time point. E) Time spent in wall, middle, and center zones for both sexes. Repeated measures ANOVA for each zone (wall, middle, center), p= 0.2295, 0.3208, 0.5055, respectively.

Tumors in both sexes respond to a combination of chemotherapy and radiation therapy, with no differences in behavior changes

Given that cancer patients receive therapy, it is important to determine the influence of standard-of-care treatment on tumor innervation and behavior. Thus, a cohort of mice were orally implanted with MOC2-7 tumors and the following groups were assessed: untreated males, treated males,

untreated females, and treated females (n=12 per group). Mice were singly housed and subjected to baseline behavior testing prior to tumor implantation. Here, voluntary wheel running and nesting were assessed. Treatment commenced on day 14 post-tumor implantation and consisted of cisplatin (intraperitoneal injection, 5.28 mg/kg) and radiation therapy (8 Gy), standard-of-care for HNSCC, once a week for two weeks. Untreated mice received vehicle. Untreated mice were given the same anesthesia needed for radiation treatment.

Female mice responded to treatment as evidenced by significantly slowed tumor growth compared to their non-treated counterparts (Figure 7B). While untreated male mice demonstrated a similar trend, this was not statistically different from male mice receiving treatment and may reflect the smaller group size (as some mice died from non-tumor mediated causes) (Figure 7A). Consistent

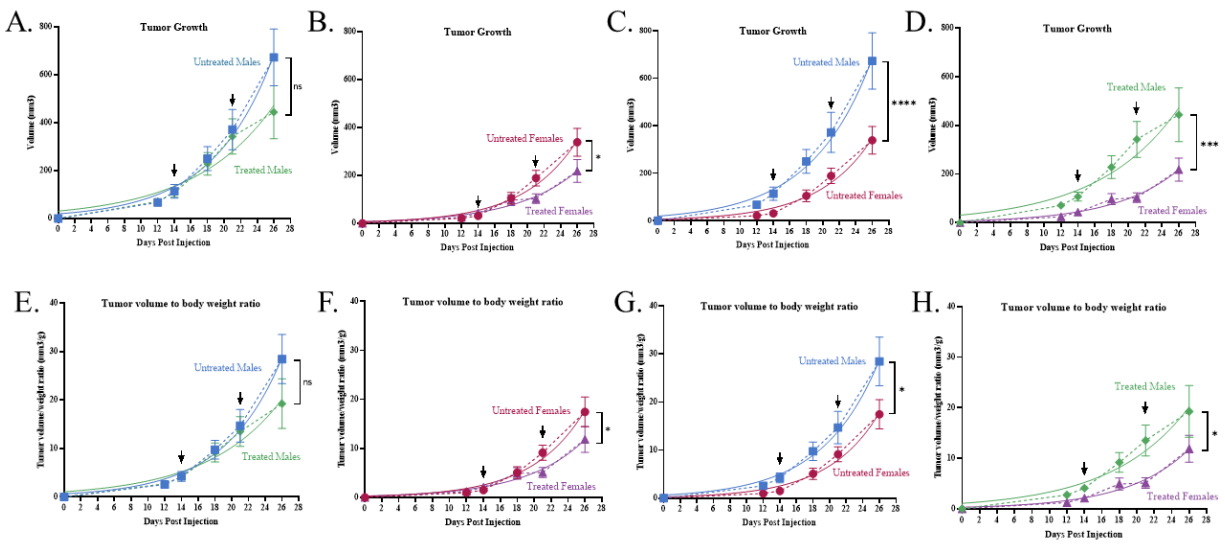

Figure 7. Tumor growth curves of untreated and treated mice. A) Growth of MOC2-7 tumors in untreated males (blue) and treated males (black) (n= 8 per group). Repeated measures ANOVA, p= 0.0931. B) Growth of MOC2-7 tumors in untreated females (red) and treated females (purple) (n= 12 per group). Repeated measures ANOVA, p= 0.0112. C) Growth of MOC2-7 tumors in untreated males and untreated females. Repeated measures ANOVA, p <0.0001. D) Growth of MOC2-7 tumors in treated males and treated females. Repeated measures ANOVA, p= 0.0002. E) Tumor volume to body weight ratio for untreated and treated males. Repeated measures ANOVA, p= 0.1529. F) Tumor volume to body weight ratio for untreated and treated females. Repeated measures ANOVA, p= 0.0321. G) Tumor volume to body weight ratio for untreated males and females. Repeated measures ANOVA, p= 0.0150. H) Tumor volume to body weight ratio for treated males and females. Repeated measures ANOVA, p= 0.0266. Tumor growth plotted (dotted lines) with non-linear exponential growth curve (solid lines). Statistical analysis by repeated measures. Arrows indicate treatment days.

with earlier data (Figure 1), tumors in female mice grew significantly slower than those in males in both untreated and treated groups (Figure 7C, D). This was true even when normalized to body weight (Figure 7F-H).

Data for nesting behavior showed all mice, regardless of sex or treatment group, declined as seen previously (Figure 6), as the disease progressed. There were no differences between sexes, regardless of treatment group (Figure 8A-D). It appeared that treatment may have restored nesting behavior in male mice, however this was not statistically significant (Figure 8C), and again, this could be due to a smaller sample size for the males. Data for voluntary running wheel suggested there may be differences between the sexes and treatment groups. All mice shared a similar decline in the total distance ran change from baseline as the disease progressed. There were no significant differences between males and females, regardless of treatment group (Figure 8E, F). There was a statistically significant difference in untreated versus treated females, with the treated group having a greater change from baseline, suggesting treatment may cause a greater decline in running behavior (Figure 8H). However, this was not statistically significant in the untreated versus treated males (Figure 8G).

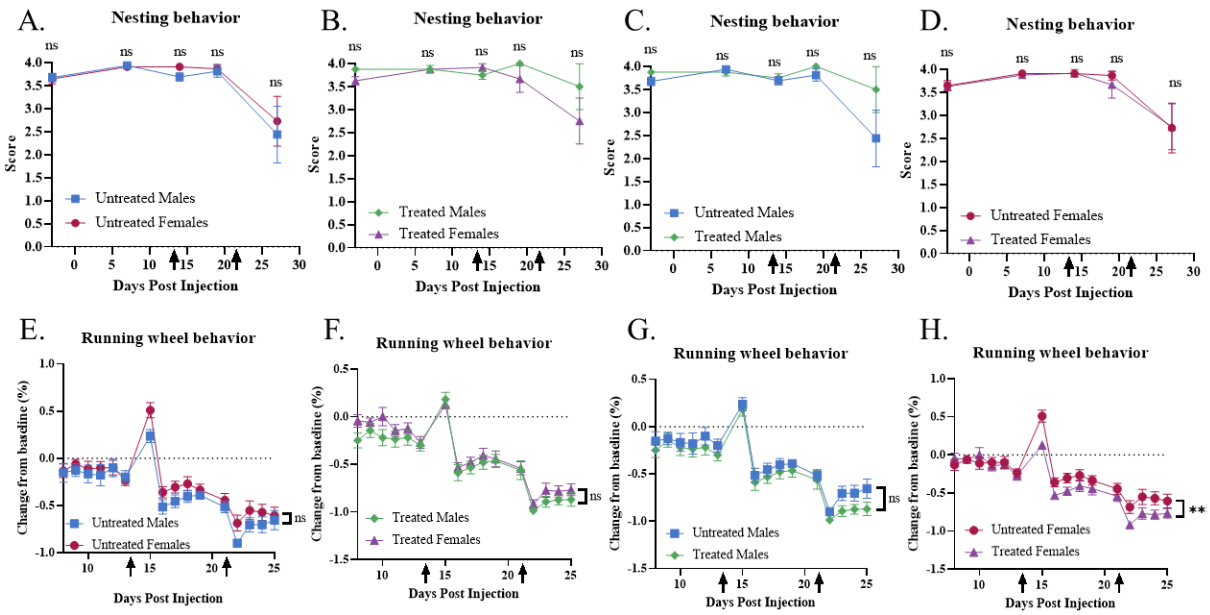

Figure 8. Nesting and voluntary running wheel behaviors of treated and untreated tumor-bearing mice. A) Nesting behavior for untreated males and females. Student's T-test with Welch's correction for baseline, days 7, 14, 19, 27, p= 0.8226, 0.7491, 0.0653, 0.7594, 0.7284, respectively. B) Nesting behavior for treated males and females. Student's T-test with Welch's correction for each time point, p= 0.0336, >0.9999, 0.2045, 0.2761, 0.3027. C) Nesting behavior for treated and untreated males. Student's T-test with Welch's correction for each time point, p= 0.0989, 0.5542, 0.6420, 0.1970, 0.2025. D) Nesting behavior for treated and untreated females. Student's T-test with Welch's correction for each time point, p= 0.8966, 0.7066, 0.9423, 0.5316, 0.9756. E) Running wheel behavior for untreated males and females. Repeated measures ANOVA, p= 0.4562. F) Running wheel behavior for treated males and females. Repeated measures ANOVA, p= 0.6652. G) Running wheel behavior for treated and untreated males. Repeated measures ANOVA, p= 0.9218. H) Running wheel behavior for treated and untreated females. Repeated measures ANOVA, p= 0.0285.

Tumors in treated mice are more densely innervated than those in untreated mice.

To assess the impact of radiochemotherapy on tumor-infiltrating nerves, following euthanasia, tumors that were harvested and sections immunofluorescently stained for the pan-neuronal marker β-III tubulin. Quantification for this staining was performed using ImageJ software for the total area of positive β-III tubulin staining. Nerve bundles were excluded from the total area. The average total area of 3 images was calculated for each tumor. Tumors from treated mice were significantly more innervated than those from untreated animals; this was true for both males and females. Treated females had the highest nerve density out of all the groups (Figure 9).

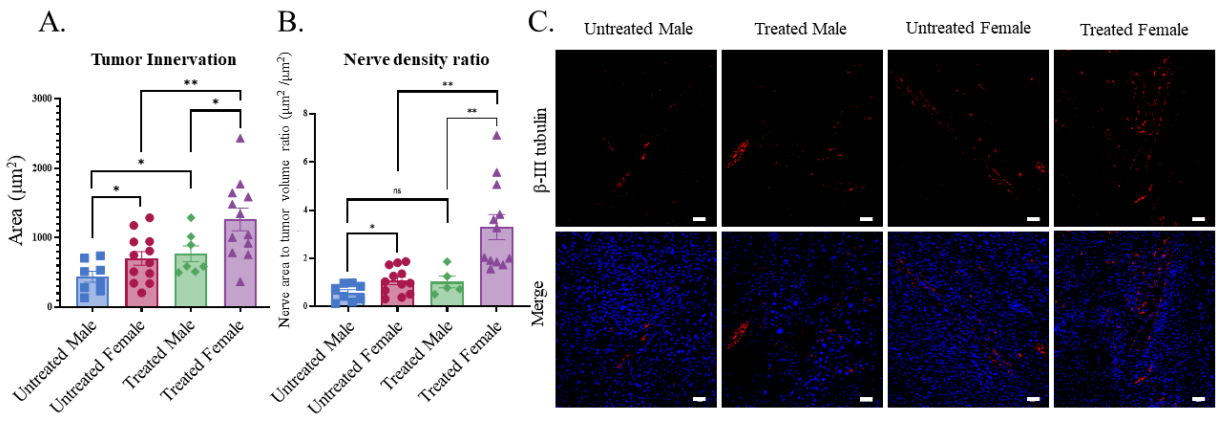

Figure 9. Tumor innervation of treated and untreated, male and female tumor-bearing mice. A) Quantification of representative images (3-4 per tumor) for total area of positive β-III tubulin staining. Student's T-test with Welch's correction for untreated males and females p= 0.0493, untreated and treated males p= 0.0360, treated males and females p= 0.0234, and untreated and treated females p= 0.0084. B) Average nerve area normalized to tumor volume. Student's T-test with Welch's correction for untreated males and females p= 0.0235, untreated and treated males p= 0.1473, treated males and females p= 0.0014, and untreated and treated females p= 0.0013. C) Representative pictomicrographs of nerve twigs and nerve bundles stained with β-III tubulin (red, arrowheads). 20x magnification, scale = 100µm.

The tumor-brain circuit does not change during treatment

To determine whether the tumor-brain connection became altered from the radiochemotherapy, a subset of animals (n=4 per group) were intra-tumorally injected with tracer 5-7 days prior to euthanasia. We found tracer positivity within the SpVc, PBN and CeA in treated and untreated animals (Figure 10). These are the same regions

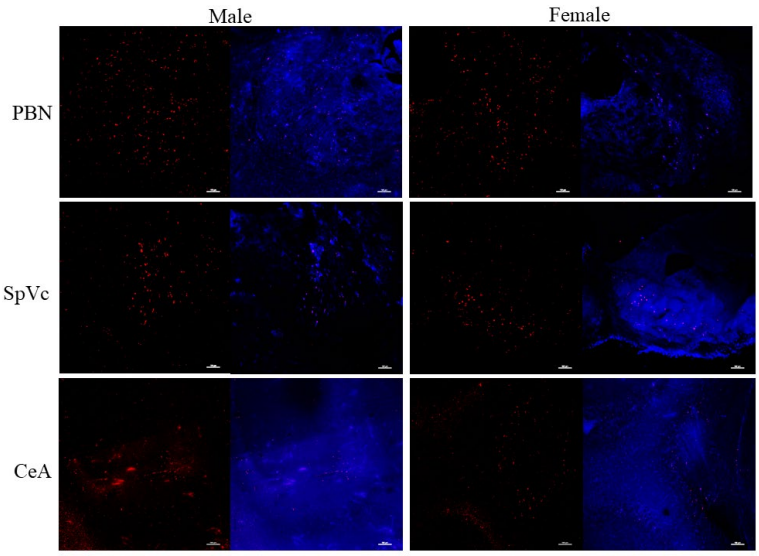

Figure 10. Neural tracer positive brain regions of treated mice. Positive WGA neural tracer found in the PBN, and SpVc, in both male and female tumor-bearing animals (n=4) treated with chemoradiotherapy. 10x magnification, scale = 100µm.

previously identified (Figure 4) [11] suggesting that combined chemoradiotherapy does not alter the tumor-brain connection.

DISCUSSION

The present studies were initiated to determine whether sex contributes to disease innervation, behavior and/or response to standard-of-care treatment in HNSCC. Using an HPV negative syngeneic cell line that grows equally well in male and female mice we show that oral MOC2-7 tumors grow significantly slower in females yet are more densely innervated than their male counterparts. Using intra-tumoral injection of a nerve tracer, we determined that the tumor-to-brain circuit does not differ between sexes indicating that the density of nerves at the tumor bed does not influence the circuit that these nerves connect to. Moreover, despite harboring more densely innervated disease, the rate and extent of behavioral decline in females was not significantly different from males. In addition, we established that chemoradiotherapy results in increased tumor innervation in male and female mice as compared to their untreated, tumor-bearing counterparts. This intriguing finding suggests that this treatment (combined cisplatin and radiation) may induce additional innervation in recurrent disease.

The presence of nerves within HNSCCs has only recently been appreciated [47, 48]. Moreover, we have demonstrated that HPV- HNSCCs are significantly more innervated than HPV+ disease and that these densely innervated tumors grow faster than their sparsely innervated counterparts [4]. Thus, we hypothesized that the slower growing tumors in female mice would be less densely innervated. To our surprise, immunofluorescent staining and quantification for nerves at the tumor bed revealed the opposite; that is, despite growing slower than males, tumors implanted in females

were significantly more innervated. It was possible that this observation was due to the smaller tumor size, however when nerve area was normalized to tumor volume, females tumors remained significantly more innervated than males. It is possible that endogenous hormones, such as estrogen, in the female mice contribute to tumor innervation, though this remains to be determined. Consistent with this hypothesis, however, studies have shown that estrogen may promote nerve regeneration [49, 50].

Using neural tracer, we have previously determined that MOC2-7 tumors in male mice are innervated by nerves of the V3 branch of the ipsilateral trigeminal (TGM) ganglion. These nerves connect to a circuit that includes the spinal nucleus of the trigeminal (SpVc), the parabrachial nucleus (PBN) and the central amygdala (CeA) [11]. We hypothesized that tumors in female mice would utilize a similar circuit. Tracer studies in tumor-bearing female mice demonstrated tracer positive neurons encompassing the same regions as tumor-bearing males. These findings indicate that despite harboring significantly greater innervation at the tumor bed, these nerves remain connected to the same circuit as males. This suggests that the greater neural density within the tumor proper is a local effect. One hypothesis which remains to be tested is that when MOC2-7 tumors are implanted in females, the hormonal and/or tumor microenvironment potentiates tumor release of exosomes, known to induce tumor innervation [47]. Increased exosome release would result in enhanced tumor innervation.

We have previously found that intra-tumoral injection of a nerve tracer allows the unambiguous identification of tumor-infiltrating neurons and the circuit(s) they connect to. Moreover, we have demonstrated that tumor-infiltrating neurons are both transcriptionally and functionally altered and that this change in neuronal activity persists in CNS neurons that they are connected to [11]. We have further shown that these cancer-induced neuronal alterations result in altered behavior [51].

Based on these findings and my identification of increased tumor innervation in female mice, I conducted behavioral testing on male and female tumor-bearing mice. Interestingly, despite harboring greater innervation at the tumor bed, the declines in behavior of female was not significantly different than males. Specifically, in the innate behaviors of nesting male and female tumor-bearing mice similarly show deficits in these behaviors starting on day 17 post-tumor implantation and this decline gets progressively worse as disease progresses. Burrowing, on the other hand, remains at baseline for both sexes until end point (day 33 post-tumor implantation) when this behavior significantly decreases at a similar rate in males and females. The difference in the timing of behavioral decline in these two measures is likely due to the influence of pain in the oral cavity and the requirement of the mouth in the behavior. Nesting requires that mice use their mouth to shred the nesting square. As tumor growth impinges on structures in the oral cavity, pain is likely associated with shredding and results in early and persistent decline in this behavior. Burrowing, on the other hand, requires removal of the medium from the burrowing tube. This is predominantly accomplished with the paws and requires little utilization of the oral cavity. Thus, tumor-bearing mice are able to complete this behavior for the majority of the experimental time. It is not until end point, when their oral tumors are quite large, that pain and potentially additional cancer-associated systemic alterations lead to decreased burrowing activity. Similarly, the open field test does not require use of the oral cavity and thus behavior declines do not occur.

To the best of our knowledge, this is the first study examining the effects of chemoradiotherapy on tumor infiltrating nerves in a head and neck cancer model. Peripheral neuropathies, whether induced by chemotherapy or radiotherapy, are common side effects found in cancer patients undergoing treatment [52-54]. Cisplatin, a standard-of-care treatment for head and neck cancers, has been shown to induce demyelination of Schwann cells, thus increasing the vulnerability of

nerves and axons to degeneration [55]. Radiation can induce oxidative stress, apoptosis, and neuroinflammation that contributes to neuropathy [56]. Though we were uncertain of what happens to intra-tumoral nerves after chemotherapy or radiation treatment, we hypothesized that chemoradiotherapy would result in decreased tumor innervation due to neuronal death and/or damage from these treatments. When we examined nerves within tumors from treated and untreated mice via immunofluorescent staining, we were surprised to find that both male and female tumors that received chemoradiotherapy were significantly more densely innervated than those from untreated mice, with females harboring the largest increase. It is likely that nerve damage induced by local radiation to the tumor induces a program of nerve regeneration which would result in enhanced innervation post-treatment. Consistent with this, a study on X-ray irradiation after peripheral nerve injury on rats concluded that low-dose irradiation had positive effects on peripheral nerve recovery, with an increase in VEGFA and GAP-43 protein levels, which are involved in axon regeneration and myelination [57]. Similarly, gamma knife irradiation, a precise, minimally invasive form of radiotherapy used to treat tumors, was found to elevate β-III tubulin protein expression, suggesting it may mediate nerve regeneration and injury repair [58]. This finding casts a shadow on chemoradiotherapy, a very commonly utilized treatment for a variety of cancers. While there is no question that this treatment slows tumor growth and that patients, at least in the short term, benefit from this therapy, our study suggests that a direct result of these treatments is the potentiation of innervation in residual and/or recurrent disease. This study also suggests that adding nerve blockers or blockers of nerve growth to this standard-of-care treatment may circumvent this influence on nerves. Moreover, based on our studies, the ability to slow tumor growth in conjunction with blocking tumor innervation is likely to slow or possibly reverse cancer-associated behavioral decline. While such a therapeutic strategy is not yet clinically

available, this study along with others, continues to indicate that targeting nerves in cancer therapies will be the next generation of therapies added to the arsenal for treating and possibly curing cancers.

CONCLUSION

These studies are the first to establish sex difference in tumor innervation in oral HNSCC. Despite harboring densely innervated disease, behavioral decline in tumor-bearing females is not different from their male counterparts. In addition, I show that the tumor-to-brain circuit is also unaltered in females as compared to males. These finding suggests that the significant increase of nerves within the local disease may be hormonally driven and that this does not alter the neuronal circuits or their impact on behavior. Importantly, I also show that standard-of-care chemoradiotherapy results in enhanced tumor innervation post-treatment. This finding strongly suggests that incorporation of nerve-targeting drugs along with standard treatments is necessary to enhance the efficacy of currently available anti-cancer therapies.

REFERENCES

1. Young, H.H., *On the Presence of Nerves in Tumors and of Other Structures in Them as Revealed by a Modification of Ehrlich's Method of "Vital Staining" with Methylene Blue.* J Exp Med, 1897. **2**(1): p. 1-12.
2. Balood, M., et al., *Nociceptor neurons affect cancer immunosurveillance.* Nature, 2022. **611**(7935): p. 405-412.
3. McIlvried, L.A., et al., *Sensory Neurotransmitter Calcitonin Gene-Related Peptide Modulates Tumor Growth and Lymphocyte Infiltration in Oral Squamous Cell Carcinoma.* Adv Biol (Weinh), 2022. **6**(9): p. e2200019.
4. Restaino, A.C., et al., *Functional neuronal circuits promote disease progression in cancer.* Sci Adv, 2023. **9**(19): p. eade4443.
5. Arakawa, H., et al., *Differences of clinical features and outcomes between male and female elderly patients in gastric cancer.* Sci Rep, 2023. **13**(1): p. 17192.
6. Mancini, M., M. Righetto, and G. Baggio, *Spotlight on gender-specific disparities in bladder cancer.* Urologia, 2020. **87**(3): p. 103-114.
7. Dong, M., et al., *Sex Differences in Cancer Incidence and Survival: A Pan-Cancer Analysis.* Cancer Epidemiol Biomarkers Prev, 2020. **29**(7): p. 1389-1397.
8. Meunier, A. and L. Marignol, *The radiotherapy cancer patient: female inclusive, but male dominated.* Int J Radiat Biol, 2020. **96**(7): p. 851-856.
9. Park, J.O., et al., *Sex Differences in the Prevalence of Head and Neck Cancers: A 10-Year Follow-Up Study of 10 Million Healthy People.* Cancers (Basel), 2022. **14**(10).
10. Fakhry, C., et al., *The prognostic role of sex, race, and human papillomavirus in oropharyngeal and nonoropharyngeal head and neck squamous cell cancer.* Cancer, 2017. **123**(9): p. 1566-1575.
11. Barr, J., et al., *Tumor-infiltrating nerves functionally alter brain circuits and modulate behavior in a mouse model of head-and-neck cancer.* bioRxiv, 2024.
12. Kunz, V., et al., *Screening for distress, related problems and perceived need for psycho-oncological support in head and neck squamous cell carcinoma (HNSCC) patients: a retrospective cohort study.* BMC Cancer, 2021. **21**(1): p. 478.
13. Lenze, N.R., et al., *Characteristics and outcomes associated with anxiety and depression in a head and neck cancer survivorship cohort.* Am J Otolaryngol, 2022. **43**(3): p. 103442.
14. Gotze, H., et al., *Depression and anxiety in long-term survivors 5 and 10 years after cancer diagnosis.* Support Care Cancer, 2020. **28**(1): p. 211-220.
15. Baraldi, J.H., et al., *Tumor Innervation: History, Methodologies, and Significance.* Cancers (Basel), 2022. **14**(8).
16. Lu, S.H., et al., *Peptidergic innervation of human esophageal and cardiac carcinoma.* World J Gastroenterol, 2003. **9**(3): p. 399-403.
17. Wacnik, P.W., et al., *Tumor-induced mechanical hyperalgesia involves CGRP receptors and altered innervation and vascularization of DsRed2 fluorescent hindpaw tumors.* Pain, 2005. **115**(1-2): p. 95-106.
18. Lindsay, T.H., et al., *Pancreatic cancer pain and its correlation with changes in tumor vasculature, macrophage infiltration, neuronal innervation, body weight and disease progression.* Pain, 2005. **119**(1-3): p. 233-246.
19. Barr, J.L., et al., *Intra-Tumoral Nerve-Tracing in a Novel Syngeneic Model of High-Grade Serous Ovarian Carcinoma.* Cells, 2021. **10**(12).

20. Barsouk, A., et al., *Epidemiology, Risk Factors, and Prevention of Head and Neck Squamous Cell Carcinoma.* Med Sci (Basel), 2023. **11**(2).
21. Vigneswaran, N. and M.D. Williams, *Epidemiologic trends in head and neck cancer and aids in diagnosis.* Oral Maxillofac Surg Clin North Am, 2014. **26**(2): p. 123-41.
22. Ramqvist, T. and T. Dalianis, *An epidemic of oropharyngeal squamous cell carcinoma (OSCC) due to human papillomavirus (HPV) infection and aspects of treatment and prevention.* Anticancer Res, 2011. **31**(5): p. 1515-9.
23. Ramqvist, T. and T. Dalianis, *Oropharyngeal cancer epidemic and human papillomavirus.* Emerg Infect Dis, 2010. **16**(11): p. 1671-7.
24. Boguna, N., L. Capdevila, and E. Jane-Salas, *Relationship of human papillomavirus with diseases of the oral cavity.* Med Clin (Barc), 2019. **153**(4): p. 157-164.
25. Lewis, A., et al., *The New Face of Head and Neck Cancer: The HPV Epidemic.* Oncology (Williston Park), 2015. **29**(9): p. 616-26.
26. Shen, W., N. Sakamoto, and L. Yang, *Cancer-specific mortality and competing mortality in patients with head and neck squamous cell carcinoma: a competing risk analysis.* Ann Surg Oncol, 2015. **22**(1): p. 264-71.
27. Mitchell, A.J., et al., *Prevalence of depression, anxiety, and adjustment disorder in oncological, haematological, and palliative-care settings: a meta-analysis of 94 interview-based studies.* Lancet Oncol, 2011. **12**(2): p. 160-74.
28. Shim, E.J., et al., *Prevalence, correlates, and impact of depressive and anxiety disorder in cancer: Findings from a multicenter study.* Palliat Support Care, 2018. **16**(5): p. 552-565.
29. Singh, P., et al., *Real-world study of the impact of recurrent/metastatic squamous cell carcinoma of the head and neck (R/M SCCHN) on quality of life and productivity in Europe.* BMC Cancer, 2021. **21**(1): p. 854.
30. Watts, S., et al., *Depression and anxiety in ovarian cancer: a systematic review and meta-analysis of prevalence rates.* BMJ Open, 2015. **5**(11): p. e007618.
31. Yadav, P., et al., *Prevalence of depressive disorders among head-and-neck cancer patients: A hospital-based, cross-sectional study.* Indian J Psychiatry, 2019. **61**(4): p. 409-414.
32. Rieke, K., et al., *Depression and survival in head and neck cancer patients.* Oral Oncol, 2017. **65**: p. 76-82.
33. Barber, B., et al., *Depression and Survival in Patients With Head and Neck Cancer: A Systematic Review.* JAMA Otolaryngol Head Neck Surg, 2016. **142**(3): p. 284-8.
34. Jansen, F., et al., *Depressive symptoms in relation to overall survival in people with head and neck cancer: A longitudinal cohort study.* Psychooncology, 2018. **27**(9): p. 2245-2256.
35. Kuba, K., et al., *Risk for depression and anxiety in long-term survivors of hematologic cancer.* Health Psychol, 2019. **38**(3): p. 187-195.
36. Mazul, A.L., et al., *Gender and race interact to influence survival disparities in head and neck cancer.* Oral Oncol, 2021. **112**: p. 105093.
37. Judd, N.P., et al., *ERK1/2 regulation of CD44 modulates oral cancer aggressiveness.* Cancer Res, 2012. **72**(1): p. 365-74.
38. Deacon, R.M., *Assessing nest building in mice.* Nat Protoc, 2006. **1**(3): p. 1117-9.
39. Deacon, R.M., *Burrowing in rodents: a sensitive method for detecting behavioral dysfunction.* Nat Protoc, 2006. **1**(1): p. 118-21.
40. Kraeuter, A.K., P.C. Guest, and Z. Sarnyai, *The Open Field Test for Measuring Locomotor Activity and Anxiety-Like Behavior.* Methods Mol Biol, 2019. **1916**: p. 99-103.

41. Goh, J. and W. Ladiges, *Voluntary Wheel Running in Mice.* Curr Protoc Mouse Biol, 2015. **5**(4): p. 283-290.
42. Huang, D., et al., *Nerve fibers in breast cancer tissues indicate aggressive tumor progression.* Medicine (Baltimore), 2014. **93**(27): p. e172.
43. March, B., et al., *Tumour innervation and neurosignalling in prostate cancer.* Nat Rev Urol, 2020. **17**(2): p. 119-130.
44. Ni, B., et al., *Crosstalk Between Peripheral Innervation and Pancreatic Ductal Adenocarcinoma.* Neurosci Bull, 2023. **39**(11): p. 1717-1731.
45. Shao, J.X., et al., *Autonomic nervous infiltration positively correlates with pathological risk grading and poor prognosis in patients with lung adenocarcinoma.* Thorac Cancer, 2016. **7**(5): p. 588-598.
46. Su, Y., et al., *Identification of lung innervating sensory neurons and their target specificity.* Am J Physiol Lung Cell Mol Physiol, 2022. **322**(1): p. L50-L63.
47. Madeo, M., et al., *Cancer exosomes induce tumor innervation.* Nat Commun, 2018. **9**(1): p. 4284.
48. Amit, M., et al., *Loss of p53 drives neuron reprogramming in head and neck cancer.* Nature, 2020. **578**(7795): p. 449-454.
49. Smith, P.G., M. George, and S. Bradshaw, *Estrogen promotes sympathetic nerve regeneration in rat proximal urethra.* Urology, 2009. **73**(6): p. 1392-6.
50. Islamov, R.R., et al., *17Beta-estradiol stimulates regeneration of sciatic nerve in female mice.* Brain Res, 2002. **943**(2): p. 283-6.
51. Tilley, E., et al., *"It is unbearable to breathe here": air quality, open incineration, and misinformation in Blantyre, Malawi.* Front Public Health, 2023. **11**: p. 1242726.
52. Staff, N.P., et al., *Chemotherapy-induced peripheral neuropathy: A current review.* Ann Neurol, 2017. **81**(6): p. 772-781.
53. Chen, A.M., et al., *Brachial plexus-associated neuropathy after high-dose radiation therapy for head-and-neck cancer.* Int J Radiat Oncol Biol Phys, 2012. **84**(1): p. 165-9.
54. Zajaczkowska, R., et al., *Mechanisms of Chemotherapy-Induced Peripheral Neuropathy.* Int J Mol Sci, 2019. **20**(6).
55. Wang, X., et al., *Platinum-based chemotherapy induces demyelination of Schwann cells in oral squamous cell carcinoma treatment.* Toxicol Appl Pharmacol, 2023. **481**: p. 116751.
56. Azzam, P., et al., *Radiation-induced neuropathies in head and neck cancer: prevention and treatment modalities.* Ecancermedicalscience, 2020. **14**: p. 1133.
57. Jiang, B., et al., *X-ray irradiation has positive effects for the recovery of peripheral nerve injury maybe through the vascular smooth muscle contraction signaling pathway.* Environ Toxicol Pharmacol, 2017. **54**: p. 177-183.
58. Yagasaki, Y., et al., *Gamma knife irradiation of injured sciatic nerve induces histological and behavioral improvement in the rat neuropathic pain model.* PLoS One, 2013. **8**(4): p. e61010.
59. Allen Reference Atlas – Mouse Brain [brain atlas]. Available from atlas.brain-map.org.